J|A|C|S COMMUNICATIONS

Published on Web 09/29/2009

Preparation of ^{14}C-Labeled Multiwalled Carbon Nanotubes for Biodistribution Investigations

Dominique Georgin, Bertrand Czarny, Magali Botquin, Martine Mayne-L'Hermite, Mathieu Pinault, Brigitte Bouchet-Fabre, Marie Carriere, Jean-Luc Poncy, Quang Chau, Rémy Maximilien, Vincent Dive,* and Frédéric Taran*

CEA, IBITECS, SCBM and SIMOPRO, CEA, IRAMIS, SPAM and SCM, Gif sur Yvette, F-91191, France, and CEA, IRCM, SREIT, Bruyères le Châtel, F-91680, France

Received August 17, 2009; E-mail: frederic.taran@cea.fr; vincent.dive@cea.fr

Multiwalled carbon nanotubes (MWNTs) are currently produced by the industry for multiple actual and future commercial applications, and consequently their potential health impact has been the subject of intense research particularly over the past 5 years. One of the main current concerns is related to the needle-like fiber shape of carbon nanotubes (NTs) that might induce asbestos-like pathogenicity.[1] Exploration of the *in vivo* biodistribution and pharmacokinetics of MWNTs with approaches offering the highest threshold in detection is therefore of prime importance. Although several studies have been carried out on pristine single-walled carbon nanotubes (SWNTs),[2] information concerning the biodistribution of nonmodified MWNTs is still lacking. Most current research has been based on the anchoring of radiolabeled molecules or radionuclide/chelate complexes on the NT surface.[3] However, such chemical modification might affect the *in vivo* clearance of NTs. In the present paper we describe a new method that allows the ^{14}C-labeling of purified MWNTs without modifying their structure, as well as the results of a preliminary biodistribution study in rats.

MWNTs are generally provided by companies as raw or as purified NTs (low iron content). Many classical purification methods, such as those involving acidic treatments, generate carboxylic acid functions in MWNTs.[4] Based on this finding, we devised a radiolabeling approach, through a three-step process, that allows carbon isotope exchange of the CO_2H moiety. The designed strategy is presented in Scheme 1 on 9-anthracen carboxylic acid **1** that was used as a model substrate for the development of the process. The anthracene moiety of this compound should mimic the aromatic network of MWNTs and provides a fluorescent signal that can be exploited.

Scheme 1. Proposed Labeling Strategy

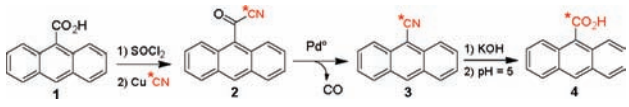

The first step of the process involves the formation of ^{14}C-labeled aroyl cyanides from a classical reaction of Cu^{14}CN with aroyl chlorides. The second step corresponds to a palladium-catalyzed decarbonylation of the aroyl cyanides into the corresponding ^{14}C-labeled nitriles. This particular reaction has been only sporadically described[5] and therefore represents the key step of the process that requires optimization efforts. Hydrolysis of the so-formed labeled nitriles into carboxylic acids should then afford ^{14}C-MWNTs that are identical to the MWNT starting material. To study the decarbonylation of aroyl cyanides, we carried out a series of more than 100 reaction conditions by varying the palladium source, the solvent, and the presence of additives (see Supporting Information) that were rapidly screened thanks to the fluorescent properties of **3**. From these screening experiments appeared $Pd(PPh_3)_4$ as the most effective palladium source and CsF as a crucial additive (Table 1).

Table 1. Optimization of the Decarbonylation Reaction of Aroyl Cyanides

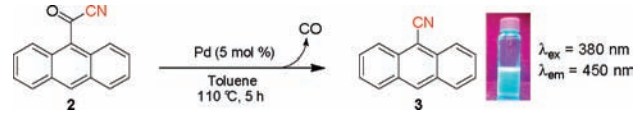

entry	Pd catalyst	additive (1 equiv)	yields (%)[a]
1	$Pd(OAc)_2$-*tert*Bu_3P[b]	–	6
2	$Pd(OAc)_2$-*n*Bu_3P[b]	–	2
3	$Pd(OAc)_2$-Ph_3P[b]	–	22
4	$Pd(OAc)_2$-DPPE[b]	–	23
5	$Pd(OAc)_2$-(*o*-tolyl)$_3P$[b]	–	5
6	$Pd(OAc)_2$-Ph_3As[b]	–	0
7	$PdCl_2(PPh_3)_2$	–	0
8	$Pd_2(dba)_3$	–	3
9	$Pd(PPh_3)_4$	–	31
10	$Pd(PPh_3)_4$	TBAF	11
11	$Pd(PPh_3)_4$	KF	65
12	$Pd(PPh_3)_4$	CsF	**99**

[a] Yields were determined by fluorescence measurements of product **3**. [b] 7.5% mol of ligands were used.

We then investigated the preparation of ^{13}C-labeled 9-anthracene carboxylic acid from its ^{12}C-analogue **1** according to Scheme 1 and using the above optimized decarbonylation reaction. Compound **4** was obtained in three steps with a reasonable global yield (52%) and an excellent isotopic enrichment (98%). The formation of aroyl cyanide **2** was the limiting step in terms of efficiency (58% yield) although the decarbonylation and hydrolysis steps proceeded with almost quantitative yields. This validated labeling process was then applied to MWNTs produced in our institute by an aerosol-assisted CVD process as previously described.[6] The iron catalyst was removed, and the MWNTs were shortened by acidic treatments (average length and diameter: 10 μm and 40 nm, respectively). Each step of the labeling process was followed by careful repeated washing to eliminate noncovalent radioactivity. Radioactive counting was used to estimate the efficiency of the labeling process (Scheme 2). After the first step (i.e., formation of α-keto nitrile), a specific activity of 0.99 MBq/mg was found. A control experiment carried out without $SOCl_2$, therefore avoiding the formation aroyl chlorides, afforded nonradioactive MWNTs. Step 2 was carried out under the optimized conditions presented in Table 1 followed by specific basic treatments to convert the remaining labeled α-keto nitriles into cold carboxylic acids. A control experiment (without

10.1021/ja906319z CCC: $40.75

the Pd catalyst) proved that the elimination of nonreacted α-keto nitriles was efficient. At the end of this process a 2-fold lower specific activity was obtained suggesting a 50% yield in the decarbonylation reaction. Finally, alkaline hydrolysis afforded the desired ^{14}C-MWNTs with a specific activity of 0.45 MBq/mg corresponding to a $^{14}C/^{12}C$ ratio of 3/1000. These results have been confirmed by surface nitrile measurements using X-ray photoelectron microscopy (XPS) conducted on samples issued from each step of the process (see Supporting Information). Further characterization of the ^{14}C-MWNTs by transmission electron microscopy (TEM) showed no significant change in their size and shape after the labeling process.

Scheme 2. ^{14}C-Labelled MWNT Preparation

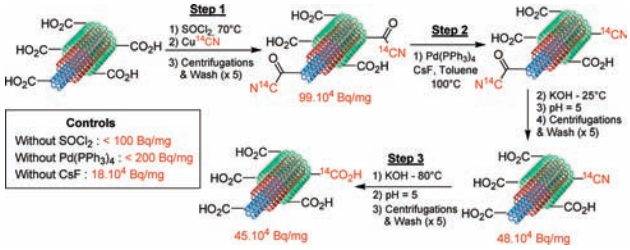

These ^{14}C-labeled MWNTs were used for preliminary *in vivo* biodistribution studies in rats. ^{14}C-MWNTs in rat serum (1 mg/mL) were sonicated until the formation of a stable suspension. TEM analysis of this suspension showed that the ^{14}C-MWNTs were shortened by this protocol (Figure 1A and B) but without loss of radiolabeling according to controls. Three groups of rats ($n = 6$) were intravenously injected with 0.35 mg of ^{14}C-MWNTs (0.15 MBq) and sacrificed 1, 7, and 14 days later. Blood and urine, as well as organs, were collected after sacrifice. The quantitative determination of the radioactivity in fluids and tissue sections were performed with a radioimager (Figure 1C).

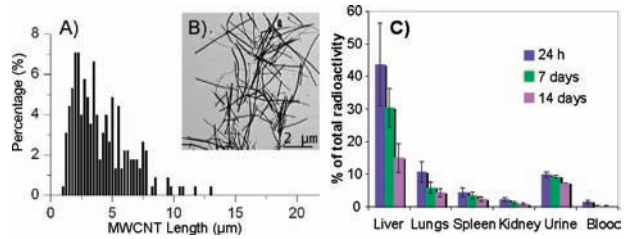

Figure 1. (A) Length characterization, (B) TEM picture, and (C) biodistribution of ^{14}C-MWNT after i.v. injection.

The ^{14}C-MWNTs were rapidly cleared from blood and distributed into organs, with a prominent liver uptake. Lungs, spleen, and kidneys were the other targeted organs; no radioactivity was detected in brain, heart, bones, stomach, and muscle. Given the ^{14}C-labeling level reported in this study and the threshold of the radioimager used for the ^{14}C detection (0.02 cpm/mm^2), up to 10 pg of ^{14}C-MWNTs can be detected. A focus on the ^{14}C-MWNT distribution within liver and lungs revealed radioactive hot spots of several μm that were shown to correspond to dark cluster by optical microscopy analysis (Figure 2). This observation suggests that ^{14}C-MWNTs accumulate in the liver and lungs under aggregates, leading to slow elimination from these organs.

In summary, we report a convenient method for the ^{14}C-labeling of purified MWNTs. Recent investigations conducted in our laboratory proved that the presented method is general and can be successfully applied to a panel of commercially available SWNTs, Hipco, and MWNTs (see Supporting Information). Since many reported molecular anchorings use the CO_2H functions present in NTs, the present method offers an interesting way to obtain radiolabeled starting nanomaterials that can be further functionalized for desired properties. Radiolabeling with a long-life radioactive nucleus like ^{14}C will make it possible to critically assess for long time periods (6 months) the biopersistence of NTs in any organs after animal exposure, as well as the possible crossing of the pulmonary barrier by NTs after inhalation, a critical safety concern for humans in the working place.

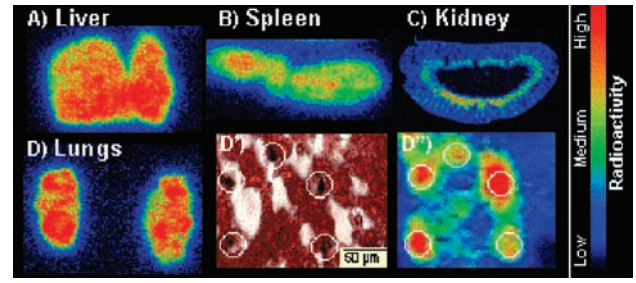

Figure 2. Tissue radioimaging in liver (A), lungs (D, D″), spleen (B), kidney (C), and optical microscopy in lungs (D′) of ^{14}C-MWNT 24 h postinjection.

Acknowledgment. This work was supported by a program of interdisciplinary research called "Nanoscience" developed by the CEA. The authors thank Dr. P. Jegou for help in XPS analysis.

Supporting Information Available: Complete analytical data of anthracene derivatives and screening results. Detailed experimental procedures of NT labeling including characterization (XPS, TEM, etc.) data and in vivo experiments. This material is available free of charge via the Internet at http://pubs.acs.org.

References

(1) Poland, C. A.; Duffin, R.; Kinloch, I.; Maynard, A.; Wallace, W. A. H.; Seaton, A.; Stone, V.; Brown, S.; MacNee, W.; Donaldson, K. *Nat. Nanotechnol.* **2008**, *3*, 423–429.

(2) (a) Cherukuri, P.; Gannon, C. J.; Leeuw, T. K.; Schmidt, H. K.; Smalley, R. E.; Curley, S. A.; Weisman, R. B. *Proc. Natl. Acad. Sci. U.S.A.* **2006**, *103*, 18882–18886. (b) Leeuw, T. K.; Reith, R. M.; Simonette, R. A.; Harden, M. E.; Cherukuri, P.; Tsyboulski, D. A.; Beckingham, K. M.; Weisman, R. B. *Nano Lett.* **2007**, *7*, 2650–2654.

(3) (a) Deng, X.; Jia, G.; Wang, H.; Sun, H.; Wang, X.; Yang, S.; Wang, S.; Wang, T.; Liu, Y. *Carbon* **2007**, *45*, 1419–1424. (b) Wang, H.; Wang, J.; Deng, X.; Sun, H.; Shi, Z.; Gu, Z.; Liu, Y.; Zhaoc, Y. *J. Nanosci. Nanotechnol.* **2004**, *4*, 1019–1024. (c) Singh, R.; Pantarotto, D.; Lacerda, L.; Pastorin, G.; Klumpp, C.; Prato, M.; Bianco, A.; Kostarelos, K. *Proc. Natl. Acad. Sci. U.S.A.* **2006**, *103*, 3357–3362. (d) Liu, Z.; Cai, W.; He, L.; Nakayama, N.; Chen, K.; Sun, X.; Chen, X.; Dai, H. *Nat. Nanotechnol.* **2007**, *2*, 47–52.

(4) See for example: (a) Liu, J.; Rinzler, A. G.; Dai, H.; Hafner, J. H.; Bradley, R. K.; Boul, P. J.; Lu, A.; Iverson, T.; Shelimov, K.; Huffman, C. B.; Rodriguez-Macias, F.; Shon, Y.-S.; Lee, T. R.; Colbert, D. T.; Smalley, R. E. *Science* **1998**, *280*, 1253–1256. (b) Dillon, A. C.; Gennett, T.; Jones, K. M.; Alleman, J. L.; Parilla, P. A.; Heben, M. J. *Adv. Mater.* **1999**, *11*, 1354–1358. (c) Duesberg, G. S.; Blau, W.; Byrne, H. J.; Muster, J.; Burghard, M.; Roth, S. *Synth. Met.* **1999**, *103*, 2484–2485. (d) Holzinger, M.; Hirsch, A.; Bernier, P.; Duesberg, G. S.; Burghard, M. *Appl. Phys. A* **2000**, *70*, 599–602. (e) Duesberg, G. S.; Muster, J.; Krstic, V.; Burghard, M.; Roth, S. *Appl. Phys. A* **1998**, *67*, 117–119.

(5) (a) Murahashi, S.-I.; Naota, T.; Nakajima, N. *J. Org. Chem.* **1986**, *51*, 898–901. (b) Brown, R. F. C.; Eastwood, F. W.; Kissler, B. E. *Tetrahedron Lett.* **1988**, *29*, 6861–6864. (c) Brown, R. F. C.; Eastwood, F. W.; Kissler, B. E. *Aust. J. Chem.* **1989**, *42*, 1435–1445.

(6) Pinault, M.; Pichot, V.; Khodja, H.; Launois, P.; Reynaud, C.; Mayne-L'Hermite, M. *Nano Lett.* **2005**, *5*, 2394–2398.

JA906319Z